Mechanism of the Verwey transition in magnetite

Przemysław Piekarz,[1] Krzysztof Parlinski,[1] and Andrzej M. Oleś[1,2]

[1] *Institute of Nuclear Physics, Polish Academy of Sciences, Radzikowskiego 152, PL-31342 Kraków, Poland*
[2] *Max-Planck-Institut für Festkörperforschung, Heisenbergstrasse 1, D-70569 Stuttgart, Germany*

(Dated: February 6, 2008)

By combining *ab initio* results for the electronic structure and phonon spectrum with the group theory, we establish the origin of the Verwey transition in Fe_3O_4. Two primary order parameters with X_3 and Δ_5 symmetries are identified. They induce the phase transformation from the high-temperature cubic to the low-temperature monoclinic structure. The on-site Coulomb interaction U between $3d$ electrons at Fe ions plays a crucial role in this transition — it amplifies the coupling of phonons to conduction electrons and thus opens a gap at the Fermi energy.
Published in Phys. Rev. Lett. **97**, *156402 (2006).*

PACS numbers: 71.30.+h, 71.38.-k, 64.70.Kb, 75.50.Gg

The discovery of the remarkable discontinuous drop of the electrical conductivity by two orders of magnitude in magnetite (Fe_3O_4) below the Verwey transition (VT) at $T_V = 122$ K [1] triggered intensive studies of its microscopic origin which have been continued for more than six decades. Verwey suggested explaining it by a metal-insulator transition due to the reduction of electron mobility caused by ordering of Fe^{3+} and Fe^{2+} ions below T_V. In spite of great experimental effort, however, the existence of ionic-like charge ordering at $T < T_V$ could not be confirmed, and the origin of the VT in magnetite remains still puzzling [2].

Magnetite is a ferrimagnetic spinel with anomalously high critical temperature $T_c \simeq 860$ K. Hence, it is viewed as an ideal candidate for room temperature spintronic applications. It crystalizes in the inverse spinel cubic structure, $Fd\bar{3}m$, with two types of Fe sites: the tetrahedral A sites and the octahedral B ones, see Ref. [3]. Below T_c, Fe_3O_4 is magnetically ordered with antiparallel moments at A and B sites. Within the commonly used ionic picture A sites are occupied by Fe^{3+} ions, and B sites are occupied randomly by Fe^{3+} and Fe^{2+} ions at room temperature. The Verwey model assumes a purely electronic mechanism of the VT, leading below T_V to ordering of Fe^{2+} and Fe^{3+} ions in B-chains, along [110] and $[1\bar{1}0]$ directions, respectively. Anderson [4] argued that the charge ordering in a form of a charge density wave, is stabilized by interionic electrostatic energy, where each B-tetrahedron consists of two Fe^{2+} and two Fe^{3+} ions. This picture was studied in the Hubbard-like model with interatomic $d-d$ Coulomb interactions [5], but was not confirmed by nuclear magnetic resonance and Mössbauer measurements [6]. While recent resonant soft X-ray scattering suggests charge-orbital ordering within the oxygen $2p$ states [7] and a cooperative Jahn-Teller effect [8], the microscopic mechanism of the VT remains controversial.

There are also other arguments against simple ionic mechanism of the VT. Firstly, the replacement of oxygen O^{16} by O^{18} isotope increases T_V by a few degrees [9], indicating that the transition cannot be purely electronic. Secondly, signals in diffuse neutron scattering observed above T_V at $\mathbf{k}_\Delta = (0, 0, \frac{1}{2})$, halfway between Γ and X points with $\mathbf{k}_X = (0, 0, 1)$, and equivalent points of the reciprocal lattice [10] (in units of $\frac{2\pi}{a}$, where a is the cubic lattice constant), change into Bragg peaks below T_V. The intensity of critical scattering was succesfully calculated on the basis of the transverse acoustic (TA) phonon mode with the Δ_5 symmetry. Further neutron studies discovered diffuse scattering with large intensities close to Γ and X points, and the dominant component of X_3 symmetry [11]. Other observations from Raman [12], X-ray [13] and nuclear inelastic scattering measurements [14] suggest that phonons play an essential role in the VT. But phonons alone cannot explain the metal-insulator nature of the transition either. Actually, if they alone were responsible, a phonon soft mode would have been found for the cubic phase, while the present *ab initio* calculations do not imply such a soft mode behavior.

The purpose of this Letter is to resolve the above controversies and to demonstrate a cooperative scenario of the VT. Following the pioneering work of Ihle and Lorenz [15], who considered weak intersite Coulomb interactions [16], we argue that a combination of local Coulomb interactions between $3d$ electrons and the electron-phonon (EP) coupling is the key feature responsible for the observed VT. Before presenting the evidence we recall that the monoclinic structure at low temperature [17], space group P2/c, with unit cell close to $a/\sqrt{2} \times a/\sqrt{2} \times 2a$, was observed using the high resolution neutron and synchrotron X-ray diffraction [3]. Having P2/c symmetry of the low temperature phase, we get a consistent description of the VT, with reflections arising below T_V at reciprocal lattice point $\mathbf{k}_\Delta$. Reflections at $\mathbf{k}_X$ and equivalent points are related to the unit cell twice shorter, namely $a/\sqrt{2} \times a/\sqrt{2} \times a$. Under typical circumstances one would select Δ_5 symmetry as a primary order parameter (OP), while X_3 as a secondary one. The symmetry analysis, however, prohibits the X_3 symmetry to be a secondary OP of Δ_5.

The electronic structures of magnetite in the cubic and

monoclinic magnetically ordered phases [3] have been obtained using *ab initio* methods. In the cubic phase, the ground state is metallic with the minority spin t_{2g} Fe(B) states at the Fermi energy [18]. The calculations for the monoclinic P2/c structure stable below T_V, performed using the LDA+U method [19], revealed the insulating state with a small gap of 0.18 eV, the value being remarkably close to the experimental one 0.15 eV [20]. The gap opening is accompanied by rather subtle charge-orbital ordering, with the charge modulation amplitude in $3d$ Fe(B) states of order $0.1e$, exactly the same as the one derived from diffraction analysis [3], and below the sensibility of other experimental techniques [6].

In order to combine the observed and computed properties of magnetite to a consistent picture of the VT, we have performed a symmetry analysis based on the group theory. For this study, we used two computer codes: the COPL [21] and ISOTROPY [22]. We recall that the high- and low-symmetry space groups for cubic and monoclinic phases [3] are Fd$\bar{3}$m and P2/c, respectively. The first observation is that there is *no* single irreducible representation (IR) of Fd$\bar{3}$m which lowers the space group Fd$\bar{3}$m directly to P2/c (see Tab. I). This means that the VT has to involve at least two OPs. Further symmetry analysis shows that two IRs, Δ_5 and X_3, acting simulataneously, reduce the space group Fd$\bar{3}$m to P2/c. Indeed, there are two symmetry reduction relationships: Fd$\bar{3}$m $\rightarrow \Delta_5 \rightarrow$ Pbcm(4) and Fd$\bar{3}$m $\rightarrow X_3 \rightarrow$ Pmna(2), where the increase of the unit cells is indicated in brackets. Common symmetry elements of Pbcm(4) and Pmna(2) form the space group P2/c(4). (We have verified that the symmetry elements are correctly located and oriented.) As a highly nontrivial result one finds that two independent IRs, Δ_5 and X_3, give two primary OPs of the VT. Moreover, the $\Gamma_5^+ = T_{2g}$ IR could also be involved in the VT.

TABLE I: List of OPs (IR) from the parent space group Fd$\bar{3}$m (No=227) and basis $(1,0,0),(0,1,0),(0,0,1)$ to the monoclinic phase P2/c (No=13, unique axis b, choice 1), basis $(\frac{1}{2},-\frac{1}{2},0),(\frac{1}{2},\frac{1}{2},0),(0,0,2)$ and origin $(\frac{1}{4},0,\frac{1}{4})$ relative to the original face center cubic lattice. Size is the ratio of primitive low-symmetry to high-symmetry unit cell volumes. Specific relationship between components of the order parameters are not shown.

IR	size	subgroup	No
Γ_1^+ (A_{1g})	1	Fd$\bar{3}$m	227
Γ_3^+ (E_g)	1	I4$_1$/amd	141
Γ_4^+ (T_{1g})	1	C2/m	12
Γ_5^+ (T_{2g})	1	Imma	74
Γ_5^+ (T_{2g})	1	C2/m	12
X_1	2	Pmma	51
X_3	2	Pmna	53
Δ_2	4	Pcca	54
Δ_4	4	Pcca	54
Δ_5	4	Pbcm	57

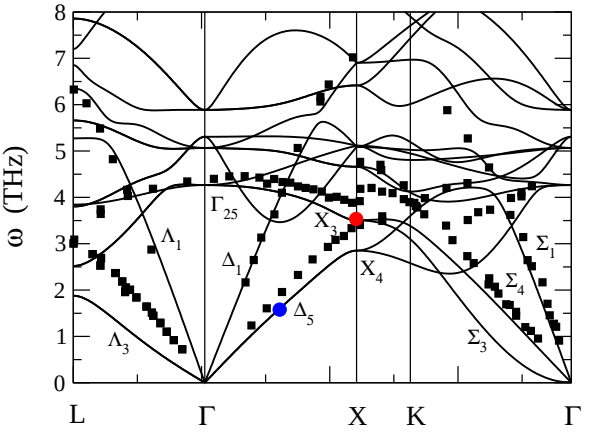

FIG. 1: (color online) Low-frequency phonon dispersion relations for cubic phase of Fe_3O_4 calculated with $U = 4$ eV and $J = 0.8$ eV. The squares show the results of neutron scattering experiment [29]. Two primary OPs are related to Δ_5 and X_3 phonons marked by circles. The high symmetry points from left to right are: $L = (\frac{1}{2},\frac{1}{2},\frac{1}{2})$, $\Gamma = (0,0,0)$, $X = (0,0,1)$, $K = (\frac{1}{4},\frac{1}{4},1)$, $\Gamma = (1,1,1)$

Its symmetry reduction relationship is Fd$\bar{3}$m $\rightarrow \Gamma_5^+ \rightarrow$ Imma(1). Symmetry elements of Imma(1) will not reduce further the symmetry of the space group P2/c(4). Thus, Γ_5^+ is a secondary OP. It represents a shear and contributes to the VT, as suggested by the observed softening of the c_{44} elastic constant [23].

The group theory tells us the order of coupling terms between the OPs. One finds that linear $\Delta_5 \otimes X_3$, linear-bilinear $\Delta_5 \otimes X_3 \otimes X_3$ and $\Delta_5 \otimes \Delta_5 \otimes X_3$ terms are forbidden by symmetry. Therefore, the fourth order coupling $\Delta_5 \otimes \Delta_5 \otimes X_3 \otimes X_3$ is the lowest one allowed by symmetry. The phase transition with two OPs has to be of the first order. The coupling between the secondary OP Γ_5^+ and X_3 is described by the linear-bilinear $\Gamma_5^+ \otimes X_3 \otimes X_3$ term. There are other IRs from Γ, X and Δ reciprocal lattice points, which could become active at the VT as secondary OPs. Although they might further diminish the ground state energy, they cannot lower the crystal symmetry.

The crystal structure of magnetite was optimized within the generalized gradient approximation (GGA) with on-site $3d$ electron interactions described by the Coulomb element U and the Hund's exchange J [24], the so-called spin-polarized GGA+U approach. The calculations were performed with the VASP code [25] on two supercells: $a\times a\times a$ and approximately $a/\sqrt{2}\times a/\sqrt{2}\times 2a$, for the cubic and monoclinic structures, respectively, with 56 atoms each. We included six valence electrons for oxygen ($2s^2 2p^4$) and eight for iron ($3d^7 4s^1$) represented by plane waves with energy cut-off 520 eV. The wave functions in the core region were obtained by the full-potential projector augmented-wave method [26]. The summation over the Brillouin zone was performed on the

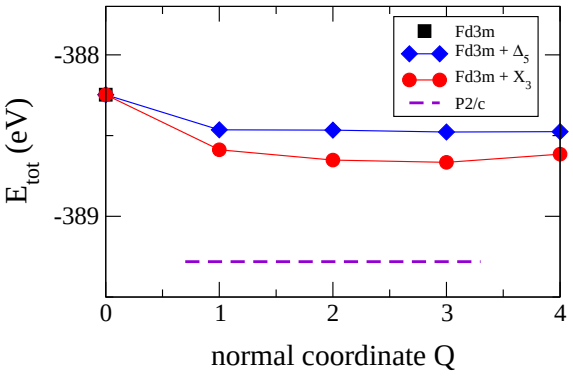

FIG. 2: (color online) Total energies $E_{\rm tot}$ per supercell of 56 atoms for the structures: cubic Fd$\bar{3}$m, cubic with superimposed phonon modes of Δ_5 at $\mathbf{k}_\Delta$ (Fd$\bar{3}$m+Δ_5), and X_3 at $\mathbf{k}_X$ (Fd$\bar{3}$m+X_3) for increasing mode amplitude Q, and for the ground state monoclinic P2/c. Parameters as in Fig. 1.

$4\times4\times4$ and $4\times4\times2$ **k**-point grids for Fd$\bar{3}$m and P2/c symmetries, respectively. For the local interactions we choose the parameters [27]: $U = 4$ eV and $J = 0.8$ eV.

Phonons were calculated only for the cubic phase, using the direct method implemented in PHONON code [28]. The Hellmann-Feynman forces were obtained for six independent displacements: two for each nonequivalent atom in positive and negative directions (with the amplitude 0.02 Å). Using the respective force constants, the dynamical matrix was constructed and diagonalized. The selected $1\times1\times1$ supercell provides exact phonon frequencies at the Γ and X points. The frequencies away from these points carry only negligible errors since the force constants decrease more than two orders of magnitude within the supercell.

The phonon dispersion curves, along the high-symmetry directions of the reciprocal space, are classified according to their IRs (Fig. 1). The longitudinal acoustic and TA modes in [001] direction correspond to one-dimensional Δ_1 and two-dimensional Δ_5 representations, respectively. As already mentioned, all phonon frequencies are real, and soft modes are absent in the cubic phase. The longitudinal acoustic modes are in a very good agreement with the neutron data measured at room temperature [29]. The discrepancies for the transverse phonons may result from the EP coupling, which effectively lowers phonon frequencies at low temperatures (as observed by diffuse scattering).

The OPs Δ_5 and X_3 could be (each one separately) a linear combination of the electronic and phononic components. In order to investigate the EP coupling for these modes, we computed the effect of applied lattice deformation, generated according to phonon polarization vectors, on the total energy and electron density of states. Among all the investigated modes with the Δ symmetry at $\mathbf{k}_\Delta$, only the TA (Δ_5) mode shows a significant coupling to electrons (presented below). At the X point, we found

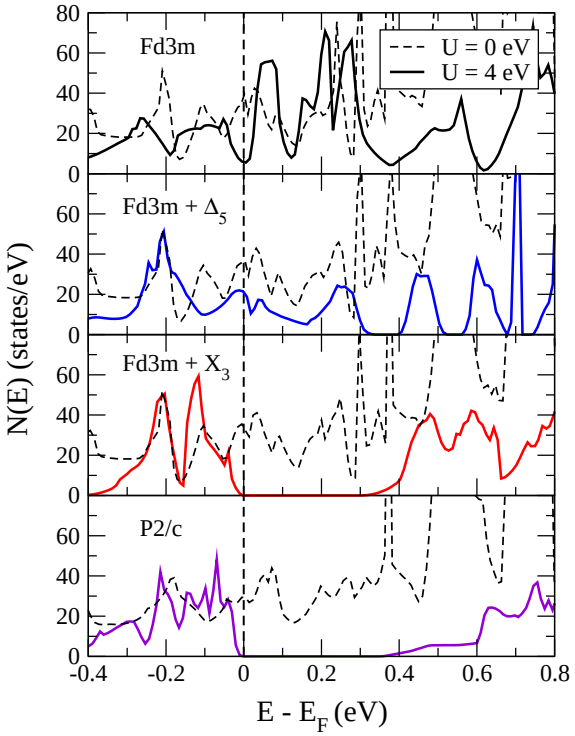

FIG. 3: (color online) Electron minority density of states for the structures of Fig. 2: cubic Fd$\bar{3}$m, cubic with superimposed phonon modes of Δ_5 at $\mathbf{k}_\Delta$ (Fd$\bar{3}$m+Δ_5) and X_3 at $\mathbf{k}_X$ (Fd$\bar{3}$m+X_3) symmetry with normal coordinate $Q = 3$, and monoclinic P2/c structures. Solid (dashed) lines correspond to $U = 4$ eV and $J = 0.8$ eV ($U = J = 0$), respectively.

a strong EP interaction for the lowest transverse optic mode with the X_3 symmetry. In contrast, the TA (X_4) and higher optic phonons couple very weakly to electrons.

When the cubic crystal is distorted by either X_3 or Δ_5 phonons, the total energy $E_{\rm tot}$ of the system decreases, indicating that these modes participate in the structural transition (Fig. 2). Note that if electrons were not involved, the ground state energies of the optimized structures distorted by phonons would have increased. The lowest energy was reached for the P2/c structure, with the optimized lattice constants and atomic positions close to these of Ref. [3], what confirms that monoclinic symmetry is stable at $T = 0$ K.

The crystal distortion which decreases the energy $E_{\rm tot}$ is directly connected with the opening of the gap at E_F in the electronic density of states (Fig. 3). For two distorted structures, and for cubic Fd$\bar{3}$m and monoclinic P2/c ones, we compare the electronic structures obtained for $U = 0$ and $U = 4$ eV. In agreement with the previous calculations [18], only down spin t_{2g} Fe(B) states contribute at E_F, and the cubic phase is metallic independently of U. For the Δ_5 deformation, magnetite remains a metal for $U = 0$, while for $U = 4$ eV one observes a significant reduction of the spectral weight above E_F, which does not yet lead to a gap. This indicates however a con-

siderable enhancement of the EP coupling for the increasing Coulomb interaction U. In the case of the X_3 mode and for $U = 4$ eV, the EP coupling is even much stronger — it opens a gap and triggers the metal-insulator transition. In contrast, a metallic phase is found for $U = 0$. Finally, for the monoclinic P2/c symmetry, the electronic state is insulating (metallic) for $U = 4$ eV ($U = 0$), in agreement with other calculations [19].

Altogether, the above results reveal a crucial role played by electron correlations in the VT. The strong Coulomb interaction U reduces the mobility of electrons in t_{2g} states, increasing their tendency towards localization. So modified electronic density responds to lattice deformation, leading to the electronic instability at the Fermi surface and to the gap opening. We emphasize that the present mechanism is novel and *does not* benefit from the Peierls-like distortions. Such a cooperative mechanism including strong electron correlations and the EP coupling was studied before [30], but the dimer-bond formation seems not to be supported experimentally [3].

As argued by Wright *et al.* [3], the lattice distortion and charge density following from diffraction analysis have predominantly character of X modulation, with additional Δ modulation. This is in perfect agreement with our result, which shows a strong coupling of the X_3 phonon mode to the electronic density. In this mode, the Fe(B) and O atoms are displaced along the diagonal [110] and [1$\bar{1}$0] directions, creating a polar deformation of B site octahedra. This lattice distortion couples to charge fluctuations on Fe(B) and O ions, inducing the diffuse scattering observed much above T_V. The observation that lattice deformation survives locally in the cubic phase [13] indicates the existence of the precursor short-range order above T_V. It is further supported by photoemission spectroscopy, consistent with the reduction of the single particle gap to ~ 0.1 eV, not closing completely at $T > T_V$ [20]. The long-range order, with larger gap, sets in at T_V due to crystal-structural transformation, as was clearly demonstrated in recent high-pressure diffraction experiment [31]. The observed charge disproportionation [7] results from the modified d-p hybridization due to the EP coupling. Finally, a gap in the magnon spectrum at $\mathbf{k}_\Delta$ point below T_V [32] indicates a large spin-phonon interaction and confirms that $\mathbf{k}_\Delta$ becomes a point on the Brillouin zone surface.

Summarizing, we have shown that the VT is driven by two primary OPs Δ_5 and X_3, which are both characterized by strong linear EP coupling, amplified by Coulomb interactions. While the cubic phase would remain metallic without this coupling, charge fluctuations of two primary OPs induced by phonons simultaneously support local lattice distortions and open a pseudogap at the Fermi energy. As a result, the condensation of both OPs leads to the monoclinic distortion below the VT, a gap develops and the conductivity is lowered. At the structural transition, the charge modulation with a tiny amplitude is stabilized, being a manifestation of the common electronic and lattice origin of this transition.

Note added. After submitting this paper new resonant X-ray scattering data were published [33] which reveal fractional charge ordering below the VT. They are fully compatible with the present explanation of the VT.

We acknowledge partial support by the European Community under FP6 contract No. NMP4-CT-2003-001516 (DYNASYNC).

[1] E.J.W. Verwey, Nature (London) **144**, 327 (1939).
[2] F. Walz, J. Phys.: Condens. Matter **14**, R285 (2002).
[3] J.P. Wright, J.P. Attfield, and P.G. Radaelli, Phys. Rev. B **66**, 214422 (2002); Phys. Rev. Lett. **87**, 266401 (2001).
[4] P.W. Anderson, Phys. Rev. **102**, 1008 (1956).
[5] J.R. Cullen and E. Callen, J. Appl. Phys. **41**, 879 (1970).
[6] J. García and G. Subías, J. Phys.: Condens. Matter **16**, R145 (2004).
[7] D.J. Huang *et al.*, Phys. Rev. Lett. **96**, 096401 (2006).
[8] D. Schrupp *et al.*, Europhys. Lett. **70**, 789 (2005).
[9] E.I. Terukov, W. Reichelt, D. Ihle, and H. Oppermann, Phys. Status Solidi B **95**, 491 (1979).
[10] Y. Fujii, G. Shirane, and Y. Yamada, Phys. Rev. B **11**, 2036 (1975).
[11] K. Siratori *et al.*, J. Phys. Soc. Jpn. **67**, 2818 (1998).
[12] R. Gupta, A.K. Sood, P. Metcalf, and J.M. Honig, Phys. Rev. B **65**, 104430 (2002).
[13] G. Subías, J. García, and J. Blasco, Phys. Rev. B **71**, 155103 (2005).
[14] B. Handke *et al.*, Phys. Rev. B **71**, 144301 (2005).
[15] D. Ihle and B. Lorenz, Philos. Mag. B **42**, 337 (1980).
[16] Intersite Coulomb interactions are largely screened by $d-p$ covalency, see: M. Imada, A. Fujimori, and Y. Tokura, Rev. Mod. Phys. **70**, 1039 (1998).
[17] M. Iizumi *et al.*, Acta Crystallogr. Sect. B **38**, 2121 (1982).
[18] Z. Zhang and S. Satpathy, Phys. Rev. B **44**, 13319 (1991).
[19] I. Leonov *et al.*, Phys. Rev. Lett. **93**, 146404 (2004); H.-T. Jeng, G.Y. Guo, and D.J. Huang, *ibid.* **93**, 156403 (2004).
[20] J.-H. Park *et al.*, Phys. Rev. B **55**, 12813 (1997).
[21] H.T. Stokes and D.M. Hatch, (2001). COPL, www.physics.byu.edu/stokesh/isotropy.html.
[22] H.T. Stokes and D.M. Hatch, (2002). ISOTROPY, stokes.byu.edu/isotropy.html.
[23] T.J. Moran and B. Lüthi, Phys. Rev. **187**, 710 (1969); H. Schwenk *et al.*, Eur. Phys. J. B **13**, 491 (2000).
[24] A.I. Liechtenstein, V.I. Anisimov, and J. Zaanen, Phys. Rev. B **52**, R5467 (1995).
[25] G. Kresse and J. Furthmüller, Comput. Mater. Sci. **6**, 15 (1996); G. Kresse and D. Joubert, Phys. Rev. B **59**, 1758 (1999).
[26] P.E. Blöchl, Phys. Rev. B **50**, 17953 (1994).
[27] J. Zaanen and G.A. Sawatzky, J. Solid State Chem. **88**, 8 (1990).
[28] K. Parlinski, Z.Q. Li, and Y. Kawazoe, Phys. Rev. Lett. **78**, 4063 (1997); K. Parlinski, Software Phonon, Cracow (2005).
[29] E.J. Samuelsen and O. Steinsvoll, Phys. Status Solidi B

61, 615 (1974).
[30] H. Seo, M. Ogata, and H. Fukuyama, Phys. Rev. B **65**, 085107 (2002).
[31] G.Kh. Rozenberg *et al.*, Phys. Rev. Lett. **96**, 045705 (2006).
[32] R.J. McQueeney *et al.*, Phys. Rev. B **73**, 174409 (2006).
[33] E. Nazarenko *et al.*, Phys. Rev. Lett. **97**, 056403 (2006).